

Pentaceno[2,3-*b*]thiophene, a Hexacene Analogue for Organic Thin Film Transistors

Ming L. Tang,[†] Stefan C. B. Mannsfeld,[‡] Ya-Sen Sun,[‡] Héctor A. Becerril,[‡] and Zhenan Bao^{*‡}

Departments of Chemistry and Chemical Engineering, Stanford University, Stanford, California 94305

Received June 10, 2008; E-mail: zbao@stanford.edu

Higher acenes with five or more fused aromatic rings are of both fundamental and practical interest. In the field of organic electronics,¹ which holds the promise of low-cost, large-area processing, acenes are exploited for their high thin film transistor charge carrier mobility.^{2,3}

Pentacene is the largest member of the unsubstituted linearly fused carbocyclic series that has been isolated and purified, with a thin film transistor mobility on par with amorphous silicon.^{4–6} Great effort has gone toward synthesizing hexacene,^{7–10} but this molecule has proven to be unstable for reasons similar to those for pentacene, where it is thought that the electron-rich central ring is susceptible to a Diels–Alder reaction with molecular oxygen.¹¹ Wudl¹² and Anthony¹³ have circumvented this by functionalizing hexacene and heptacene with bulky groups, for example tris(trimethylsilyl)silyl acetylene, obtaining solution grown single crystals. Neckers and co-workers managed to photogenerate hexacene¹⁴ and heptacene¹⁵ in a polymer matrix, allowing the spectroscopic signatures of these elusive molecules to be recorded. To retain the linear fused architecture of hexacene, higher thienoacenes containing five to seven fused units have been synthesized.^{16–18} However, these thienoacenes are not as conjugated as their carbocyclic analogues, and with the exception of dibenzothieno bisbenzothiophene¹⁹ (which was synthesized as a mixture of three isomers), no thin film transistor (TFT) has been reported.

In this communication, we present a hexacene-like molecule containing six linearly fused rings, as well as its TFT properties. To our knowledge, this is the most conjugated acene-based molecule that so far has been used for TFT purposes. Expanding on our previous work,²⁰ we wondered if pentaceno[2,3-*b*]thiophene, **1**, which is pentacene fused with a terminal thiophene ring could be made. The synthesis is shown in Scheme 1. The precursor quinone,

mass spectrometry (MS). The structure of **3** is assigned based on MS data, the lower absorption in the long wavelength region, and the fact that the central rings should be most reactive.¹¹ Molecules **1**, **2**, and **3** are too insoluble for proton NMR or other standard characterization techniques. However, they have different colors and markedly different UV–vis spectra (see Supporting Information, SI, Figure S1). We then used 2,3-dichloro-5,6-dicyanobenzoquinone (DDQ) to oxidize the mixture back to the target compound (see SI). This gave **1**, which was sublimed once in a three-zone furnace at high vacuum (10^{−6}Torr) to give the target compound, a purple-black powder. This molecule is fully characterized by mass spectroscopy and elemental analysis.

To obtain the highest occupied molecular orbital (HOMO) level of **1**, we performed cyclic voltammetry under argon gas in 0.1 M tetrabutylammonium hexafluorophosphate in *o*-dichlorobenzene (*o*-DCB) at 100 °C. We measured the HOMO of **1** to be −4.87 eV (see SI), which is close to P3HT. From the long wavelength absorption edge in UV–vis in *o*-DCB (inset of Figure 1), we find

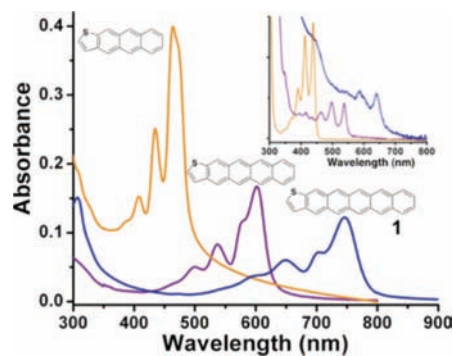
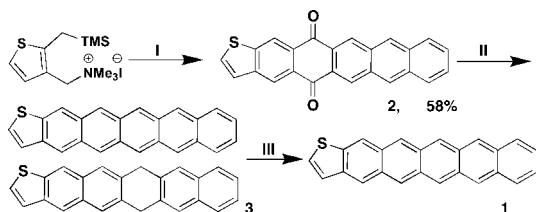


Figure 1. UV–vis absorption spectrum of 45nm thin films of anthra[2,3-*b*]thiophene, tetraceno[2,3-*b*]thiophene, and pentaceno[2,3-*b*]thiophene, **1**, evaporated on quartz under device conditions. Inset: The UV–vis of these molecules in *o*-DCB at RT.

the HOMO–LUMO gap is 1.75 eV, and the LUMO to be −3.15 eV. Figure 1 plots the UV–visible absorption spectrum of 45nm thin films evaporated under device conditions of anthra[2,3-*b*]thiophene, tetraceno[2,3-*b*]thiophene and pentaceno[2,3-*b*]thiophene, while the inset plots the UV–vis of these molecules in *o*-DCB. As can be seen, the λ_{\max} of the three molecules in *o*-DCB increases by ~100nm as an additional benzene ring is added, from 438nm to 536nm, and 640nm respectively. This trend holds in the 45nm thin films. From this, we calculate the optical bandgap of **1** in thin film to be 1.58 eV, compared to 1.96 eV for tetraceno[2,3-*b*]thiophene and 2.51 eV anthra[2,3-*b*]thiophene.

Ultraviolet photoelectron spectroscopy (UPS) in air gave the thin film an ionization potential of 4.63 eV. The stability of a 20 nm thin film of **1** was monitored over a period of 4 days in ambient (laboratory air and fluorescent lights) by UV–vis (Figure S7). The

Scheme 1. Synthesis of Pentaceno[2,3-*b*]thiophene, **1**^a



^a (i) 1,4-Naphthoquinone, tetrabutylammonium fluoride (TBAF), DMF, 100 °C; (ii) Al, CBr₄, HgCl₂, CyOH, reflux; (iii) DDQ, dioxane, reflux.

2, was made by a Diels–Alder reaction with 1,4-naphthoquinone.²¹ However, reduction of this quinone, **2**, with the standard aluminum-cyclohexanol complex gave a brown mixture of the target compound, **1**, and the over-reduced byproduct, **3**, as indicated by

[†] Department of Chemistry.

[‡] Department of Chemical Engineering.

decay in the long wavelength peak at 750 nm can be fitted with a half-life ($T_{1/2}$) of 127 min as shown in Figure S6. The second-order exponential decay is consistent with the diffusion of triplet oxygen into the film,²² reacting with **1**. Comparing this to pentacene's $T_{1/2}$ of 140 min¹¹ when irradiated by 254 nm UV light, evidently **1** is less stable than pentacene but more stable than hexacene¹⁴ and heptacene.¹⁵ This is consistent with the general observation that substituting the terminal benzene ring on a linear acene with a fused thiophene ring makes the molecule more stable than its carbocyclic counterpart.²⁰ It is interesting to note that all these linear acenes adopt the herringbone packing in thin film, as shown by grazing incidence X-ray diffraction (GIXD) in Table S2, the unit cell differing mainly by the c -axis increasing with each successive addition of a benzene ring from 12.34 to 15.16²³ to 17.89 Å.

Organic TFTs were made from **1** in the top-contact geometry by evaporation under high vacuum on bare SiO₂ and octadecyltrimethoxysilane (OTS) treated SiO₂, and also at two substrate temperatures, RT and 60 °C. Some devices were fabricated and measured entirely in nitrogen, while others were exposed to ambient for 20 min before gold deposition during the shadow mask placement. The latter were measured both in nitrogen (to minimize oxidation) and in air. For every condition, 6–10 devices were averaged. Devices fabricated and measured entirely in nitrogen showed the highest on current (0.6 mA), the highest average and maximum mobility of 0.457 and 0.574 cm²/V s, respectively, on OTS treated surfaces at 60 °C, and the lowest gate leakage current on SiO₂. For the same conditions, devices measured in nitrogen but exposed to air prior to gold deposition had an average mobility of 0.391 cm²/V s. Devices measured in air showed lower mobility on the same order of magnitude, registering up to a 50% decrease (see SI) in the average mobilities. The differences between the three batches of devices are summarized in Figure S8. Figure 2 also plots

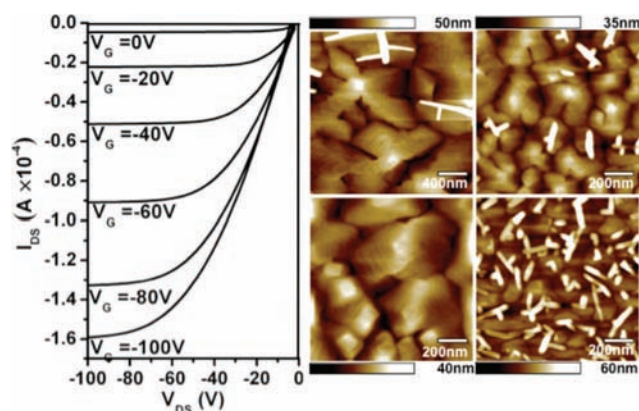


Figure 2. A characteristic OTFT output curve for **1**, on OTS treated SiO₂, and the corresponding AFM for SiO₂ (top) and OTS/SiO₂ (bottom) on substrate temperatures of 60 °C (left) and RT (right).

an output curve characteristic of the best performing devices from Table 1. **1** forms dendritic grains, similar to the characteristic morphology of pentacene and tetraceno[2,3-*b*]thiophene, as shown in Figure 2. As expected, there is an increase in mobility from RT to 60 °C that corresponds with an increase in grain size in AFM images (see Figures S3–4) and an increase in crystallinity as indicated by the out-of-plane X-ray diffraction (XRD) that shows up to six orders of diffraction (see Figure S5).

Table 1. OTFT Data for **1**, with the Mobility, μ , On/Off Ratio, and Threshold Voltage, V_T , at Substrate Temperatures RT and 60 °C^a

		SiO ₂	OTS/SiO ₂
RT	μ (cm ² /V s)	0.0677 ± 0.05	0.276 ± 0.09
	on/off	2E+03	1E+06
	V_T (V)	0	+10
60 °C	μ (cm ² /V s)	0.222 ± 0.06	0.391 ± 0.07
	on/off	7E+02	3E+03
	V_T (V)	+10	+20

^a These were top-contact devices, channel length, $L = 100 \mu\text{m}$, $W/L = 20$, and Au electrodes, measured in nitrogen, but exposed to air for 20 min for gold deposition.

In conclusion, we have synthesized, isolated, and purified a hexacene-like molecule containing six linearly fused rings. In the thin film, its UV–vis absorption extends beautifully into the near-infrared region. OTFTs were successfully prepared and exhibit high mobility and thin film growth characteristic of pentacene.

Acknowledgment. The authors thank Dr. Toshihiro Okamoto for synthetic suggestions. M.L.T. acknowledges a Kodak graduate fellowship while Z.B. thanks AFSOR and GCEP for financial support.

Supporting Information Available: Synthetic details, X-ray OOP d -spacings and graphs, AFM images, UV–vis of the decay of the thin film, the unit cells from GIXD, characteristic OTFT curves (including hysteresis) and a cyclic voltammogram. This material is available free of charge via the Internet at <http://pubs.acs.org>.

References

- (1) Bao, Z.; Locklin, J. *Organic Field-Effect Transistors (Optical Science and Engineering Series)*; CRC Press: Boca Raton, FL, 2007.
- (2) Anthony, J. E. *Chem. Rev.* **2006**, *106*, 5028–5048.
- (3) Murphy, A. R.; Frechet, J. M. J. *Chem. Rev.* **2007**, *107*, 1066–1096.
- (4) Nelson, S. F.; Lin, Y. Y.; Gundlach, D. J.; Jackson, T. N. *Appl. Phys. Lett.* **1998**, *72*, 1854–1856.
- (5) Klauk, H.; Halik, M.; Zschieschang, U.; Schmid, G.; Radlik, W.; Weber, W. *J. Appl. Phys.* **2002**, *92*, 5259–5263.
- (6) Baude, P. F.; Ender, D. A.; Haase, M. A.; Kelley, T. W.; Muires, D. V.; Theiss, S. D. *Appl. Phys. Lett.* **2003**, *82*, 3964–3966.
- (7) Clar, E. *Polycyclic Hydrocarbons*; Academic Press: London, 1964; Vol. 1.
- (8) Bailey, W. J.; Liao, C. W. *J. Am. Chem. Soc.* **1955**, *77*, 992–993.
- (9) Campbell, R. B.; Trotter, J.; Monteath, J. *Acta Crystallogr.* **1962**, *15*, 289–290.
- (10) Stachell, M. P.; Stacey, B. E. *J. Chem. Soc. C* **1971**, 468–469.
- (11) Maliakal, A.; Raghavachari, K.; Katz, H.; Chandross, E.; Siegrist, T. *Chem. Mater.* **2004**, *16*, 4980–4986.
- (12) Chun, D.; Cheng, Y.; Wudl, F. *Angew. Chem., Int. Ed.* **2008**, *47*, 1–6.
- (13) Payne, M. M.; Parkin, S. R.; Anthony, J. E. *J. Am. Chem. Soc.* **2005**, *127*, 8028–8029.
- (14) Mondal, R.; Adhikari, R. M.; Shah, B. K.; Neckers, D. C. *Org. Lett.* **2007**, *9*, 2505–2508.
- (15) Mondal, R.; Shah, B. K.; Neckers, D. C. *J. Am. Chem. Soc.* **2006**, *128*, 9612–9613.
- (16) Okamoto, T.; Kudoh, K.; Wakamiya, A.; Yamaguchi, S. *Org. Lett.* **2005**, *7*, 5301–5304.
- (17) Okamoto, T.; Kudoh, K.; Wakamiya, A.; Yamaguchi, S. *Chem.—Eur. J.* **2007**, *13*, 548–556.
- (18) Zhang, X. N.; Cote, A. P.; Matzger, A. J. *J. Am. Chem. Soc.* **2005**, *127*, 10502–10503.
- (19) Sirringhaus, H.; Friend, R. H.; Wang, C.; Leuninger, J.; Müllen, K. *J. Mater. Chem.* **1999**, *9*, 2095–2101.
- (20) Tang, M. L.; Okamoto, T.; Bao, Z. N. *J. Am. Chem. Soc.* **2006**, *128*, 16002–16003.
- (21) Patney, H. K. *J. Org. Chem.* **1988**, *53*, 6106–6109.
- (22) Doremus, R. H. *Diffusion of Reactive Molecules in Solids and Melts*; John Wiley & Sons, Inc.: New York, 2002.
- (23) Yuan, Q.; Mannsfeld, S. C. B.; Tang, M. L.; Toney, M. F.; Luening, J.; Bao, Z. A. *J. Am. Chem. Soc.* **2008**, *130*, 3502–3508.

JA808142C